Design of Linear Equalizers Optimized for the Structural Similarity Index

Sumohana S. Channappayya, *Member, IEEE*, Alan Conrad Bovik, *Fellow, IEEE*, Constantine Caramanis, *Member, IEEE*, and Robert W. Heath, Jr., *Senior Member, IEEE*

Abstract—We propose an algorithm for designing linear equalizers that maximize the structural similarity (SSIM) index between the reference and restored signals. The SSIM index has enjoyed considerable application in the *evaluation* of image processing algorithms. Algorithms, however, have not been designed yet to explicitly optimize for this measure. The design of such an algorithm is nontrivial due to the nonconvex nature of the distortion measure. In this paper, we reformulate the nonconvex problem as a quasi-convex optimization problem, which admits a tractable solution. We compute the optimal solution in near closed form, with complexity of the resulting algorithm comparable to complexity of the linear minimum mean squared error (MMSE) solution, independent of the number of filter taps. To demonstrate the usefulness of the proposed algorithm, it is applied to restore images that have been blurred and corrupted with additive white gaussian noise. As a special case, we consider blur-free image denoising. In each case, its performance is compared to a locally adaptive linear MSE-optimal filter. We show that the images denoised and restored using the SSIM-optimal filter have higher SSIM index, and superior perceptual quality than those restored using the MSE-optimal adaptive linear filter. Through these results, we demonstrate that a) designing image processing algorithms, and, in particular, denoising and restoration-type algorithms, can yield significant gains over existing (in particular, linear MMSE-based) algorithms by optimizing them for perceptual distortion measures, and b) these gains may be obtained without significant increase in the computational complexity of the algorithm.

Index Terms—Equalizers, image restoration.

I. INTRODUCTION

THE mean squared error (MSE) is a popular metric used in the design of image processing algorithms ranging from quantization to restoration to quality assessment. The popularity of MSE can be largely attributed to two main reasons: amenability to analysis and a lack of competitive perceptual distortion metrics. This has been the case even though it has been shown that MSE optimal algorithms do not necessarily produce images of high visual quality [11]. Since most images are intended for human consumption, using perceptual metrics to design image processing algorithms seems natural. This has long been recognized [32] and algorithms that take into account the human visual system (HVS) in the design have been developed, e.g., image compression [9], [17], [19], [31]. Several of these solutions use modified versions of the MSE as the distortion measure such as the weighted MSE. These designs were limited by a paucity of strong perceptual distortion measures at the time, combined with the complexity of the available measures [7], [16], [25], [33].

Recent advances in full-reference image quality assessment (IQA) have resulted in the emergence of several powerful perceptual distortion measures that outperform the MSE and its variants. A nonexhaustive but significant list of these new metrics includes the SSIM Index [27], or Wang–Bovik Index and its variants [26], [29], [30], the visual information fidelity (VIF) criterion [22], [23], and the visual signal-to-noise ratio (VSNR) [5]. Despite their success in quality assessment, image processing algorithms that explicitly optimize using *state-of-the-art* perceptual distortion measures such as these have not yet been developed. The design process for most of these measures is nontrivial because of their less tractable forms compared to the MSE, e.g., the VIF computes image quality as a ratio of sum of logarithmic terms, while the SSIM index uses the expression in (7).

In this paper, the SSIM index is considered as a design criterion. The SSIM index is relatively easy to analyze, yet is highly competitive with state-of-the-art IQA algorithms. Optimizing with respect to the SSIM index was considered in [6] and [28], in a very limited context, but even these obtained significant perceptual gains compared to MSE-optimal techniques. In this paper, we design a linear equalizer optimized for the SSIM index and apply it to image denoising and restoration examples, and compare its performance to a linear MSE-optimal filter. Through these examples, we demonstrate the gain in perceptual quality obtained using the SSIM-optimal linear equalizer.

A. Problem Outline

In this paper, we propose the design of a linear equalizer optimized with respect to the SSIM index. This is a generalization of an earlier result on linear estimation for image denoising [6]. We address the general problem of equalization of wide sense stationary (WSS) processes (of which denoising is a special case), and design a length N equalizer (for any N) optimized for the SSIM index between the reference and restored processes. The definition of the SSIM index is first extended

to measure similarity between random processes via a straightforward replacement of empirical quantities by their statistical equivalents. The equalization problem is then formulated using this extended definition. The SSIM index between the reference and test signal is shown to be a nonconvex function of the equalizer coefficients. The nonconvex problem is reformulated as a quasi-convex problem by imposing parameterized linearity constraints on the equalizer coefficients, which then admits a tractable solution. The optimal solution is computed by an easy 1-D search over the linearity constraint parameter. To demonstrate its usefulness, the solution is then applied to both an image denoising problem and an image restoration problem.

B. Related Work

The problem of deconvolution and image restoration (of which denoising is a special case) has been widely researched [1], [14] and several different approaches have been studied. A broad classification of the various approaches can be found in [14]. The literature is rich with several excellent results such as regularized iterative restoration [15], space-varying iterative restoration [21], wavelet shrinkage based techniques [8], spatially adaptive wavelet-based restoration [2], the wavelet-based expectation maximization technique in [10], Gaussian scale mixture (GSM) based restoration [20], combined Fourier and wavelet techniques, such as the ForWaRD algorithm [18], to name a few.

The purpose of this paper is primarily to put forth a new design philosophy based on a perceptual criterion. Our formulation is intended to compare perceptual approaches with classical approaches to signal equalization, in order to demonstrate the proof of principle that gains in perceptual quality can be obtained. Following the classification of restoration approaches in [14], this paper falls under the category of *stochastic linear iterative* algorithms, which includes Wiener based solutions [12]. As in the Wiener solution, our solution requires knowledge of the autocorrelation function of the source. This problem is addressed by using an estimation algorithm as in [20].

C. Paper Organization

We begin by providing a brief introduction to the SSIM index in Section II and extending it to measure similarity between random processes. The problem is formulated in terms of an extended statistical definition of the SSIM index. We then illustrate its nonconvex nature and the associated issues with optimization. In Section III, the procedure used to reformulate the nonconvex optimization problem and obtain its solution is discussed. We then describe the design algorithm. The usefulness of the design algorithm is illustrated in Section IV using image denoising and restoration examples. To demonstrate the gain in perceptual quality achieved by this algorithm, the performance of the SSIM-optimal linear filter is compared to an MSE-optimal linear filter (using the image restoration example). The results are discussed in Section V and we conclude in Section VI, outlining future research directions.

II. PROBLEM FORMULATION

In this section, we discuss the system model and assumptions, describe the SSIM index, and extend its definition to handle random processes. The equalization problem is then formulated using the extended definition of the SSIM index. The problem
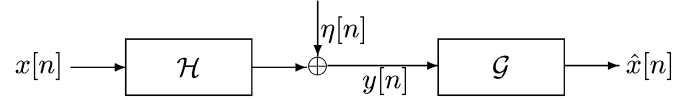

Fig. 1. Block diagram of a general linear time invariant system. In this paper, we are interested in designing the linear equalizer block $\mathcal{G}$, given the observed process $y[n]$, the LTI filter $\mathcal{H}$, and the power spectral density of the noise process $\eta[n]$ so that the SSIM index between $x[n]$ and $\hat{x}[n]$ is maximized.

is discussed both intuitively and using the algebraic form of the function being optimized.

A. System Model

The equalization problem is illustrated in Fig. 1. We assume that the input to the system $x[n]$ is a WSS process, $h[n]$ is a linear time invariant (LTI) filter known at the receiver, and the noise process $\eta[n]$ is white and its power spectral density (PSD) is know at the receiver. The following problem is considered. Given a distorted observation

$$y[n] = h[n] * x[n] + \eta[n] \tag{1}$$

of the input process $x[n]$, design a filter $g[n]$ of length N such that the SSIM index between the reference $x[n]$ and the restored process

$$\hat{x}[n] = g[n] * y[n] \tag{2}$$

is maximized. Since the standard definition of the SSIM index [27] measures similarity between deterministic signals, its definition is first extended to measure similarity between random processes in the following subsection.

B. SSIM Index

The most general form of the SSIM index defined for signal vectors $\mathbf{x}$ and $\mathbf{y}$ (in $\mathbf{R}^N$) is

$$\text{SSIM}(\mathbf{x}, \mathbf{y}) = [l(\mathbf{x}, \mathbf{y})]^\alpha [c(\mathbf{x}, \mathbf{y})]^\beta [s(\mathbf{x}, \mathbf{y})]^\gamma. \tag{3}$$

The term

$$l(\mathbf{x}, \mathbf{y}) = \frac{2\mu_x \mu_y + C_1}{\mu_x^2 + \mu_y^2 + C_1} \tag{4}$$

compares the luminance (mean) of the signals

$$c(\mathbf{x}, \mathbf{y}) = \frac{2\sigma_x \sigma_y + C_2}{\sigma_x^2 + \sigma_y^2 + C_2} \tag{5}$$

compares the contrast (variance) of the signals, and

$$s(\mathbf{x}, \mathbf{y}) = \frac{\sigma_{xy} + C_3}{\sigma_x \sigma_y + C_3} \tag{6}$$

measures the structural correlation of the signals. The quantities μ_x, μ_y are the sample means of $\mathbf{x}$ and $\mathbf{y}$, respectively, σ_x^2, σ_y^2 are the sample variances of $\mathbf{x}$ and $\mathbf{y}$, respectively, and σ_{xy} is the sample cross covariance between $\mathbf{x}$ and $\mathbf{y}$. The constants C_1, C_2, C_3 are used to stabilize the SSIM index for the case where the means and variances become very small. The parameters $\alpha > 0$, $\beta > 0$, and $\gamma > 0$, are used to adjust the relative importance of the three components.
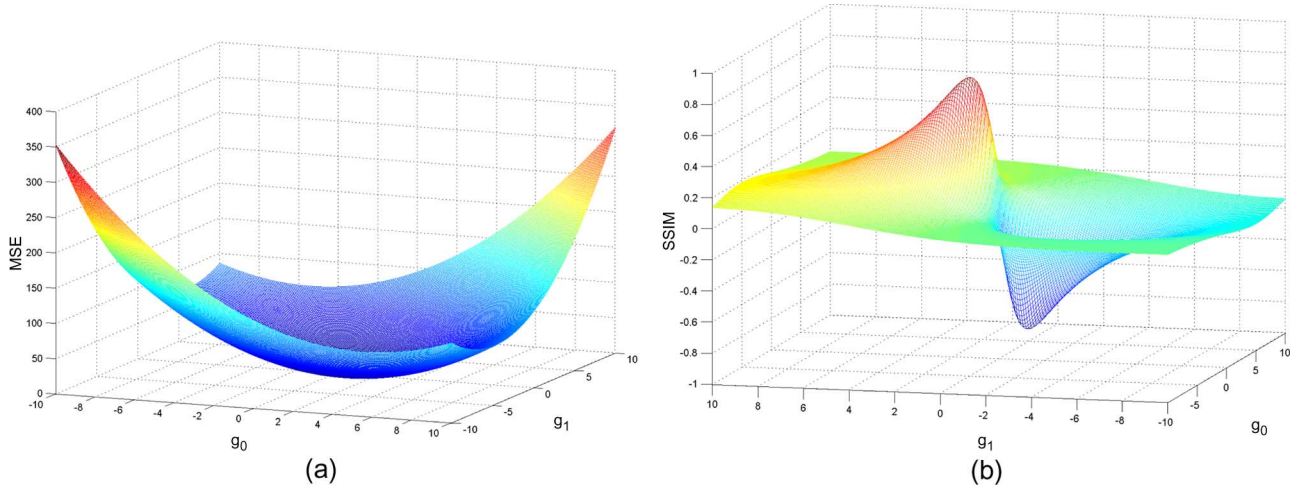
Fig. 2.   MSE and SSIM index as a function of equalizer taps $g[0], g[1]$. (a) MSE; (b) SSIM.

As in [27], we use the following simplified form of the SSIM index ($\alpha = \beta = \gamma = 1$, $C_3 = C_2/2$)

$$\text{SSIM}(\mathbf{x}, \mathbf{y}) = \left(\frac{2\mu_x\mu_y + C_1}{\mu_x^2 + \mu_y^2 + C_1} \right) \left(\frac{2\sigma_{xy} + C_2}{\sigma_x^2 + \sigma_y^2 + C_2} \right). \quad (7)$$

In image quality assessment, image sub-blocks from the reference and distorted image constitute $\mathbf{x}$ and $\mathbf{y}$, respectively. The average of the SSIM values across the image (also called mean SSIM or MSSIM) gives the final quality measure. The design philosophy of the SSIM index is to exploit the fact that natural images are highly structured, and that the measure of structural correlation (between the reference and the distorted image) is very important in deciding the overall visual quality. Further, the SSIM index measures quality locally and is able to capture local dissimilarities well. The SSIM index has been shown to correlate better with the mean opinion score (MOS) of subjective evaluation for a large set of images (relative to MSE and, hence, PSNR). In [27], a database consisting of 175 JPEG compressed images and 169 JPEG2000 compressed images at various quality levels was used to test the performance of the SSIM index. The scores were shown to correlate very well with the MOS of subjective evaluation. In [24], a larger image database (consisting of 779 images of different visual qualities) also confirmed the superior performance of the SSIM index as an IQA algorithm relative to the MSE. Though (7) has a form that is more complicated than MSE ($(\text{MSE}(\mathbf{x}, \mathbf{y}) = (1/N) \sum_{i=0}^{N-1} (x_i - y_i)^2)$), it remains analytically tractable. These features make the SSIM index attractive.

Since we work with random processes in this paper, the definition of the SSIM index must be modified accordingly. We, therefore, introduce the *statistical SSIM index* (StatSSIM index) as follows.

Definition: Given two WSS random processes $x[n]$ and $y[n]$ with means μ_x and μ_y, respectively, the statistical SSIM index is defined as

$$\text{StatSSIM}\,(x[n], y[n]) = \left(\frac{2\mu_x\mu_y + C_1}{\mu_x^2 + \mu_y^2 + C_1} \right)$$

$$\times \left(\frac{2E\left[(x[n] - \mu_x)(y[n] - \mu_y) \right] + C_2}{E\left[(x[n] - \mu_x)^2 \right] + E\left[(y[n] - \mu_y)^2 \right] + C_2} \right). \quad (8)$$

This is a straightforward extension of the pixel domain definition of the SSIM index by replacing sample means and variances with their statistical equivalents.

C. Equalization Problem

Suppose that a WSS process $x[n]$ is distorted by a linear time invariant (LTI) filter $h[n]$, then corrupted by an additive white noise process $\eta[n]$ (zero-mean): $y[n] = h[n] * x[n] + \eta[n]$. The proposed problem is the design of an equalizer $g[n]$ of length N, that maximizes the StatSSIM index between the source process $x[n]$ and the equalized (restored) process $\hat{x}[n] = g[n] * y[n]$. We can rewrite the StatSSIM index as a function of $g[n]$ using (8) as [see (9), shown at the bottom of the next page], where $\mathbf{g} = [g[0], g[1], \ldots, g[N-1]]^T$, $\mathbf{e} = [1, 1, \ldots, 1]^T$ are both length N vectors, μ_x, μ_y are the means of the source and observed processes, respectively, $\mathbf{c}_{xy} = E[(x[n] - \mu_x)(\mathbf{y} - \mathbf{e}\mu_y)]$, is the cross covariance between the source ($x[n]$) and the observed processes ($\mathbf{y} = (y[n], y[n-1], \ldots, y[n-(N-1)])^T$), σ_x^2 is the variance of the source process at zero delay, $\mathbf{K}_{yy} = E[(\mathbf{y} - \mathbf{e}\mu_y)(\mathbf{y} - \mathbf{e}\mu_y)^T]$, is the covariance matrix of size $N \times N$ of the observed process $y[n]$, and C_1, C_2 are stabilizing constants.

Our problem is then to find the optimal filter

$$\mathbf{g}^* = \arg\max_{\mathbf{g} \in \mathbb{R}^N} \text{StatSSIM}\,(x[n], \hat{x}[n]). \quad (10)$$

We assume that the blurring filter $h[n]$ (of length M) and, the power spectral density (PSD) of $\eta[n]$ is known at the receiver.

From (9), we see that the StatSSIM index is the ratio of a second degree polynomial to a fourth degree polynomial in g. A geometric feel for the function in (9) is given in Fig. 2 for a length 2 filter and is compared to the convex form of MSE. Fig. 2(b) clearly illustrates the nonconvex nature of (9). Despite these features, we show in Section III that problem (9) admits a tractable, and in particular, near closed-form solution, with a complexity that is comparable to that of the MMSE solution.

III. StatSSIM-Optimal Linear Equalization

Since the StatSSIM index is a nonconvex function of $\mathbf{g}$, local optimality conditions such as Karush–Kuhn–Tucker (KKT) cannot guarantee global optimality. In particular, any approach based on descent-type algorithms are likely to get stuck in

local optima. The approach that we take to solve this problem transforms the nonconvex problem into a quasi-convex formulation. Convex optimization problems are efficiently solvable using widely available optimization techniques and software [3], [4]. We show, moreover, that, in addition to the convex reformulation, we can obtain a near-closed form solution. In particular, we reduce the N-tap filter optimization, for *any* N, into an optimization problem over only *two* variables. Exploiting convexity properties, we can quickly search over one parameter by means of a bisection technique, thus reducing the problem to a univariate optimization problem. This last step can be quickly performed by means of an analytic solution of a simplified problem, which brings us close to the optimal value of the final variable of our optimization.

A. Problem Reformulation

Note that the first term of (9) (corresponding to the mean) is a function only of the sum of the filter coefficients $\mathbf{g}^T \mathbf{e}$. We use this property to simplify the optimization problem in (9) by constraining $\mathbf{g}^T \mathbf{e} = \alpha$. With this constraint, the optimization problem simplifies to finding

$$\left[\mathbf{g}(\alpha) = \arg\max_{\mathbf{g} \in \mathbb{R}^N} \left(\frac{2\mathbf{g}^T \mathbf{c}_{xy} + C_2}{\sigma_x^2 + \mathbf{g}^T \mathbf{K}_{yy} \mathbf{g} + C_2} \right) \right.$$
$$\left. \text{subject to} : \mathbf{g}^T \mathbf{e} = \alpha \right]. \quad (11)$$

This problem is a function of α. The overall problem is to find the highest StatSSIM index by searching over a range of α (typically in the interval $[1 - \delta, 1 + \delta]$, for a small δ). The solution to the optimization problem in (11) is presented in the following section, along with an efficient search strategy for finding α.

B. Solution

The maximization problem in (11) is still nonconvex. We convert it into a quasi-convex optimization problem as follows:

$$\mathbf{g}(\alpha) = \arg\max_{\mathbf{g} \in \mathbb{R}^N} \left(\frac{2\mathbf{g}^T \mathbf{c}_{xy} + C_2}{\sigma_x^2 + \mathbf{g}^T \mathbf{K}_{yy} \mathbf{g} + C_2} \right)$$
$$\text{subject to} : \mathbf{g}^T \mathbf{e} = \alpha,$$

$$\text{StatSSIM}\,(x[n], \hat{x}[n])$$

$$= f(\mathbf{g}) = \left(\frac{2\mu_x \mu_{\hat{x}} + C_1}{\mu_x^2 + \mu_{\hat{x}}^2 + C_1} \right) \left(\frac{2E\left[(x[n] - \mu_x)(\hat{x}[n] - \mu_{\hat{x}})\right] + C_2}{E\left[(x[n] - \mu_x)^2\right] + E\left[(\hat{x}[n] - \mu_{\hat{x}})^2\right] + C_2} \right)$$

$$= \left(\frac{2\mu_x E\left[\sum_{i=0}^{N-1} g[i]y[n-i]\right] + C_1}{\mu_x^2 + \left(E\left[\sum_{i=0}^{N-1} g[i]y[n-i]\right]\right)^2 + C_1} \right)$$

$$\times \left(\frac{2E\left[(x[n] - \mu_x)\left(\sum_{i=0}^{N-1} g[i]y[n-i] - E\left[\sum_{i=0}^{N-1} g[i]y[n-i]\right]\right)\right] + C_2}{E\left[(x[n] - \mu_x)^2\right] + E\left[\left(\sum_{i=0}^{N-1} g[i]y[n-i] - E\left[\sum_{i=0}^{N-1} g[i]y[n-i]\right]\right)^2\right] + C_2} \right)$$

(which follows from the definition of convolution)

$$= \left(\frac{2\mu_x \sum_{i=0}^{N-1} g[i]\mu_y + C_1}{\mu_x^2 + \left(\sum_{i=0}^{N-1} g[i]\mu_y\right)^2 + C_1} \right)$$

$$\times \left(\frac{2E\left[(x[n] - \mu_x)\left(\sum_{i=0}^{N-1} g[i]y[n-i] - \sum_{i=0}^{N-1} g[i]\mu_y\right)\right] + C_2}{E\left[(x[n] - \mu_x)^2\right] + E\left[\left(\sum_{i=0}^{N-1} g[i]y[n-i] - \sum_{i=0}^{N-1} g[i]\mu_y\right)^2\right] + C_2} \right)$$

(since $x[n]$ is WSS, $h[n]$ is LTI, $y[n]$ is also WSS)

$$= \left(\frac{2\mu_x \mathbf{g}^T \mathbf{e}\mu_y + C_1}{\mu_x^2 + \mathbf{g}^T \mathbf{e}\mathbf{e}^T \mathbf{g}\mu_y^2 + C_1} \right)$$

$$\times \left(\frac{2E\left[(x[n] - \mu_x)(\sum_{i=0}^{N-1} g[i](y[n-i] - \mu_y))\right] + C_2}{E\left[(x[n] - \mu_x)^2\right] + E\left[\left(\sum_{i=0}^{N-1} g[i](y[n-i] - \mu_y)\right)^2\right] + C_2} \right)$$

$$= \left(\frac{2\mu_x \mathbf{g}^T \mathbf{e}\mu_y + C_1}{\mu_x^2 + \mathbf{g}^T \mathbf{e}\mathbf{e}^T \mathbf{g}\mu_y^2 + C_1} \right) \left(\frac{2\mathbf{g}^T \mathbf{c}_{xy} + C_2}{\sigma_x^2 + \mathbf{g}^T \mathbf{K}_{yy} \mathbf{g} + C_2} \right) \quad (9)$$

```
1. Pick an initial guess of γ (say γ₀) between 0 and 1. upper_limit = 1,
   lower_limit = γ₀.
2. Evaluate the optimal filter.
3. Is γ(σ²_x + g^T K_yy g + C₂) - (2g^T c_xy + C₂) ≥ 0?
   3a. If true, is (upper_limit - lower_limit < ε)?
      3aa. If true, we have found a γ within ε of the optimal value. Exit.
      3ab. If false, set γᵢ = 0.5*(upper_limit + lower_limit),
           upper_limit = γᵢ. Goto step 2.
   3b. If false, set γᵢ = 0.5*(upper_limit + lower_limit), lower_limit = γᵢ.
       Goto step 2.
```

Fig. 3. Algorithm to search for the optimal γ.

$$\Leftrightarrow$$
$$\min : \gamma$$

subject to :
$$\begin{bmatrix} \max : & \left(\frac{2\mathbf{g}^T \mathbf{c}_{xy} + C_2}{\sigma_x^2 + \mathbf{g}^T \mathbf{K}_{yy} \mathbf{g} + C_2} \right) \leq \gamma \\ \text{subject to :} & \mathbf{g}^T \mathbf{e} = \alpha, \end{bmatrix}$$

$$\Leftrightarrow$$
$$\min : \gamma$$

subject to :
$$\begin{bmatrix} \min : & \left[\gamma \left(\sigma_x^2 + \mathbf{g}^T \mathbf{K}_{yy} \mathbf{g} + C_2 \right) - (2\mathbf{g}^T \mathbf{c}_{xy} + C_2) \right] \geq 0 \\ \text{subject to :} & \mathbf{g}^T \mathbf{e} = \alpha \end{bmatrix}. \quad (12)$$

The first step in the reformulation is the introduction of the auxiliary variable γ as an upper bound on (11). The first equivalence relation holds since minimizing γ is the same as finding the least upper bound of the function in (11). This is equal to the maximum value of the function, which exists, as seen by straightforward continuity arguments. The second equivalence relation holds since the denominator in (11) is strictly positive, allowing us to multiply through and rearrange terms. Then, γ is a true upper bound if the problem
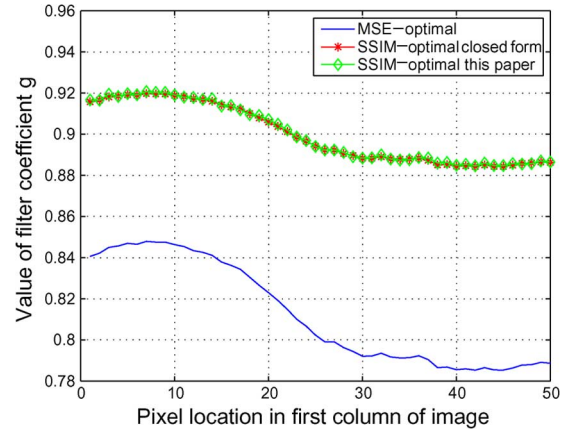
$$\begin{bmatrix} \max_{\mathbf{g} \in \mathbb{R}^N} : & \gamma \left(\sigma_x^2 + \mathbf{g}^T \mathbf{K}_{yy} \mathbf{g} + C_2 \right) - (2\mathbf{g}^T \mathbf{c}_{xy} + C_2) \\ \text{subject to :} & \mathbf{g}^T \mathbf{e} = \alpha \end{bmatrix} \quad (13)$$

has a non-negative optimal value. Since the objective function is a linear term minus a convex quadratic, it is concave. The constraint is affine and, thus, convex. Therefore, the overall problem is convex, and can be solved by introducing a Lagrange multiplier λ and applying the first-order sufficiency conditions

$$\nabla_g \left\{ \gamma \left(\sigma_x^2 + \mathbf{g}^T \mathbf{K}_{yy} \mathbf{g} + C_2 \right) - (2\mathbf{g}^T \mathbf{c}_{xy} + C_2) + \lambda (\mathbf{g}^T \mathbf{e} - \alpha) \right\} = 0. \quad (14)$$

Solving for $\mathbf{g}$ and λ, and denoting them $\mathbf{g}(\alpha)$, $\lambda(\alpha)$ to emphasize their dependence on α, we have

$$\mathbf{g}(\alpha) = \frac{1}{2\gamma} \mathbf{K}_{yy}^{-1} (2\mathbf{c}_{xy} - \lambda(\alpha)\mathbf{e})$$

$$\lambda(\alpha) = \frac{1}{\mathbf{e}^T \mathbf{K}_{yy}^{-1} \mathbf{e}} \left(2\mathbf{c}_{xy}^T \mathbf{K}_{yy}^{-1} \mathbf{e} - 2\gamma\alpha \right). \quad (15)$$

Fig. 4. Comparison of the denoising filter coefficient from this paper's result with the Wiener filter and the result in [6] at noise variance $\sigma_n^2 = 625$.

The optimal γ can then be computed in $O(\log(1/\epsilon))$ iterations using a standard bisection procedure. Such an algorithm is summarized in Fig. 3. In this procedure, the threshold ϵ determines the tightness of the bound γ. In other words, the solution obtained using this technique will be within ϵ of the optimal solution. The efficiency of the algorithm can be improved using better search techniques.

C. Search for α

The solution in (15) maximizes the function in (12) to give $\mathbf{g}(\alpha)$, i.e., it is still a function of α. The optimal solution to (9) is found by searching over α. The search is over a bounded 1-D interval and is, therefore, easy to perform. We present two ways to speed up this search.

The first is to simply initialize α to the sum of the filter coefficients of the MSE-optimal filter, i.e., $\alpha_{\text{init}} = \mathbf{g}_{\text{mse}}^T \mathbf{e}$. The second is a heuristic technique that was found to work better than the first in all our experiments with natural images. In this technique, α is initialized to the sum of the filter coefficients of a structure-optimal filter. By structure-optimal filter, we mean a filter that optimizes only the structure term in the StatSSIM index without any constraints on the mean. This would yield a filter that is optimal with respect to one of the two terms in the StatSSIM index (9). In the following, the structure-optimal filter is derived.
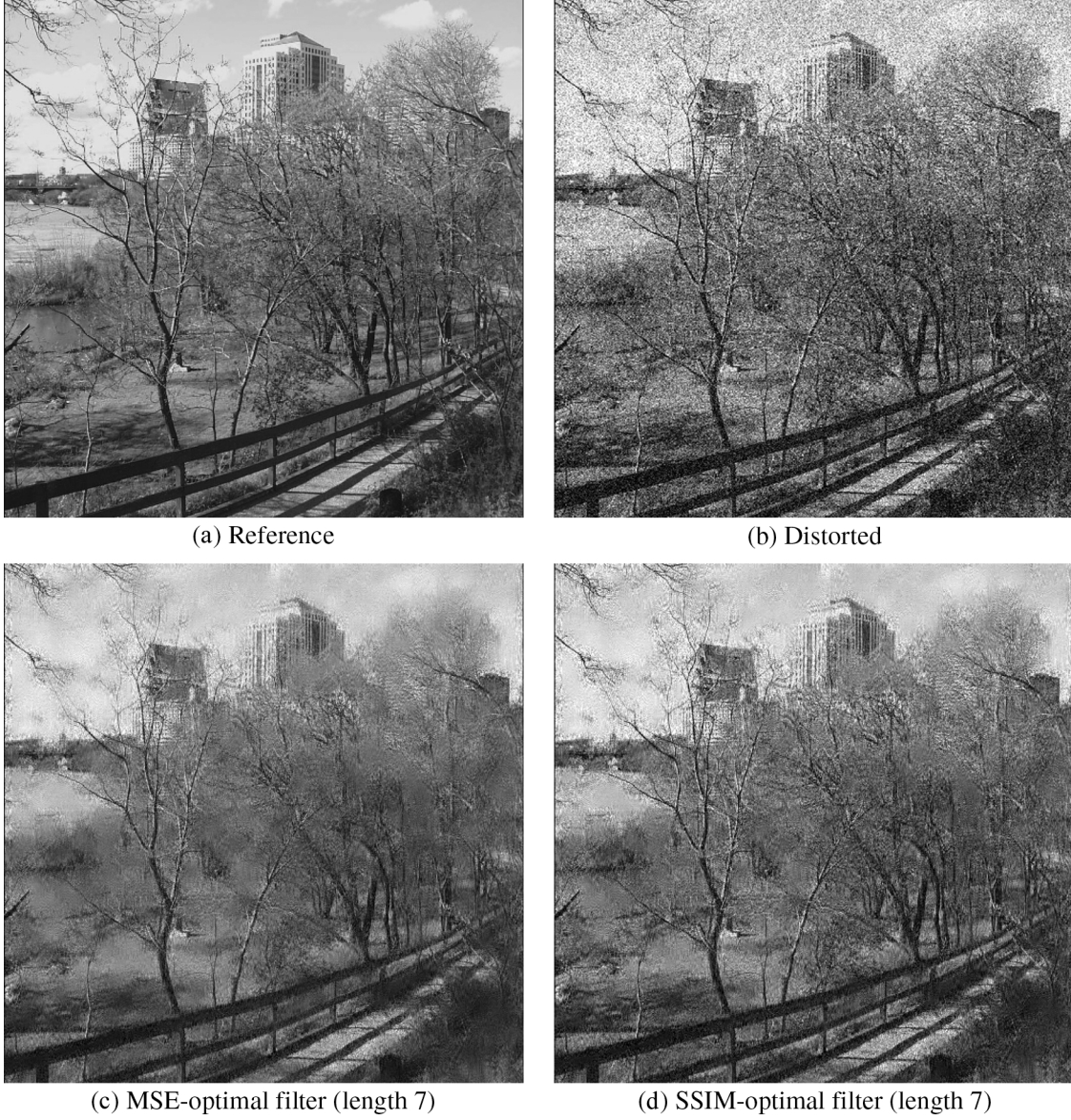
(a) Reference

(b) Distorted

(c) MSE-optimal filter (length 7)

(d) SSIM-optimal filter (length 7)

Fig. 5. *Denoising example 1*: Img0039.bmp from the "City of Austin" database. (a) Original image. (b) Distorted image with $\sigma_{\mathrm{noise}} = 35$, $\mathrm{MSE} = 1226.3729$, $\mathrm{SSIM\ index} = 0.5511$. (c) Image denoised with a 7-tap MSE-optimal filter, $\mathrm{MSE} = 436.6929$, $\mathrm{SSIM\ index} = 0.6225$. (d) Image denoised with a 7-tap SSIM-optimal filter, $\mathrm{MSE} = 528.0777$, $\mathrm{SSIM\ index} = 0.6444$.

Following the notation in Section II-C, our goal is to find a filter $\mathbf{g}^*_{\mathrm{struct}}$ such that

$$
\begin{aligned}
\mathbf{g}^*_{\mathrm{struct}} &= \arg\max_{\mathbf{g} \in \mathbb{R}^N} \mathrm{Structure}\,(x[n], \hat{x}[n]) \\
&= \left(\frac{2E\left[(x[n] - \mu_x)\,(\hat{x}[n] - \mu_{\hat{x}}) \right] + C_2}{E\left[(x[n] - \mu_x)^2 \right] + E\left[(\hat{x}[n] - \mu_{\hat{x}})^2 \right] + C_2} \right) \\
&= \left(\frac{2\mathbf{g}^T \mathbf{c}_{xy} + C_2}{\sigma_x^2 + \mathbf{g}^T \mathbf{K}_{yy}\mathbf{g} + C_2} \right).
\end{aligned} \tag{16}
$$

This problem has the same form as (11) and, thus, can be quickly solved using the optimization technique given above. The optimal solution is

$$
\mathbf{g}^*_{\mathrm{struct}} = \frac{1}{\gamma_{\mathrm{struct}}} (\mathbf{K}_{yy})^{-1} \mathbf{c}_{xy} \tag{17}
$$

and so the initial value of α is

$$
\alpha_{\mathrm{init}} = \mathbf{e}^T \mathbf{g}^*_{\mathrm{struct}}. \tag{18}
$$

The value of γ_{struct} is computed using the same algorithm as in Section III-B, and this value is potentially different from the γ in Section III-B.

D. Comparison With Denoising Solution

Section III-B provides a near closed-form solution for the linear equalization problem optimized for the StatSSIM index for a general equalizer length N. For the no-blur case the solution becomes

$$
\mathbf{g}(\alpha) = \frac{1}{2\gamma} \mathbf{K}_{yy}^{-1} \left(2\mathbf{c}_{xx} - \lambda(\alpha)\mathbf{e} \right)
$$

$$
\lambda(\alpha) = \frac{1}{\mathbf{e}^T \mathbf{K}_{yy}^{-1} \mathbf{e}} \left(2\mathbf{c}_{xx}^T \mathbf{K}_{yy}^{-1}\mathbf{e} - 2\gamma\alpha \right) \tag{19}
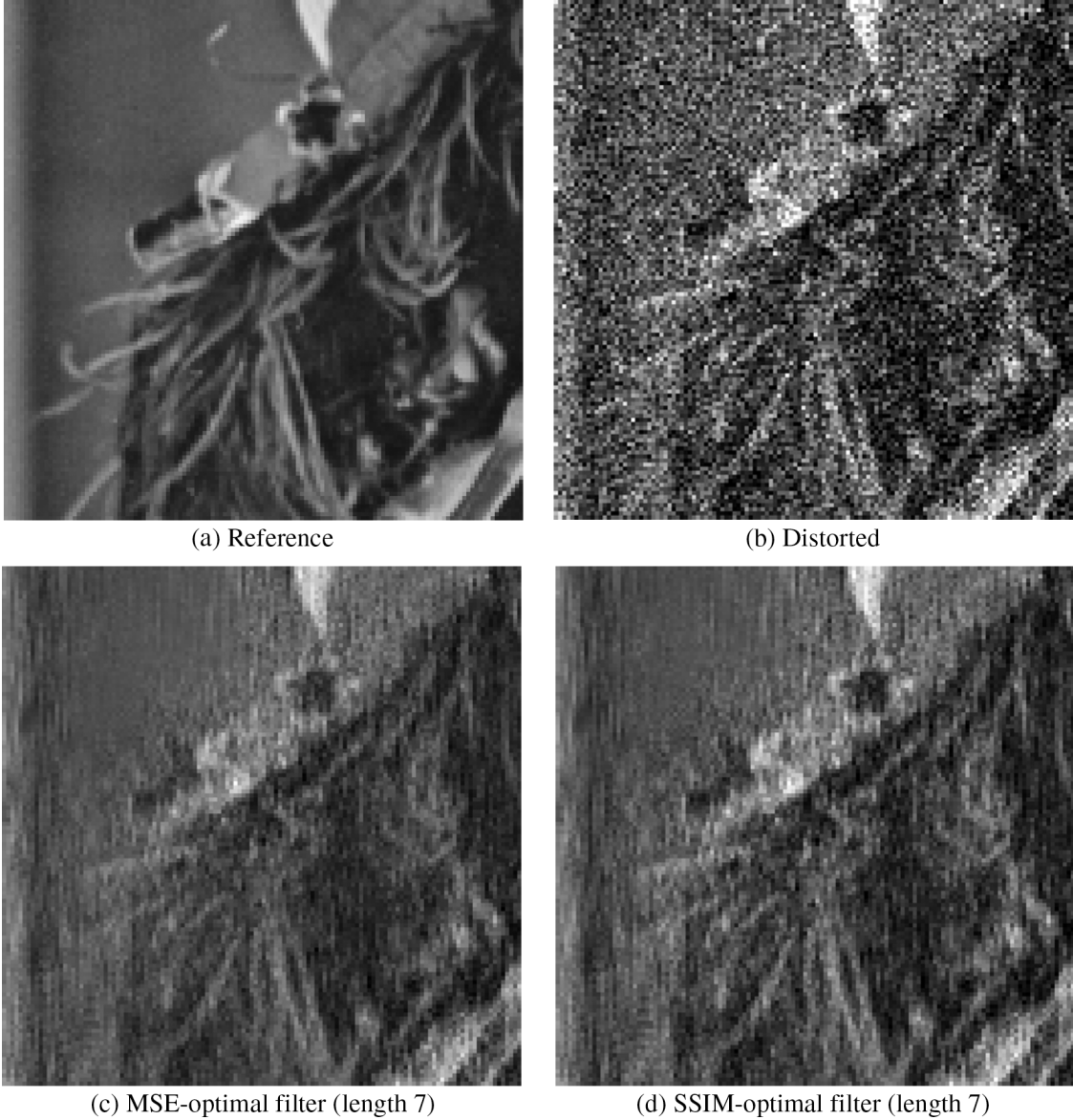$$

(a) Reference

(b) Distorted

(c) MSE-optimal filter (length 7)

(d) SSIM-optimal filter (length 7)

Fig. 6. *Denoising example 2*: (a) Original image. (b) Distorted image with $\sigma_{\text{noise}} = 40$, $\mathrm{MSE} = 1639.3132$, $\mathrm{SSIM\ index} = 0.541485$. (c) Image denoised with the a 7-tap MSE-optimal filter, $\mathrm{MSE} = 383.3375$, $\mathrm{SSIM\ index} = 0.734963$. (d) Image denoised with a 7-tap SSIM-optimal filter, $\mathrm{MSE} = 455.2577$, $\mathrm{SSIM\ index} = 0.753917$.

where $\mathbf{c}_{xx} = E[(x[n] - \mu_x)(\mathbf{x} - \mathbf{e}\mu_x)]$, $\mathbf{x} = (x[n], x[n - 1], \ldots, x[n - (N - 1)])^T$. In [6], a closed-form SSIM-optimal denoising solution was presented for a one tap filter. We compare the closed-form solution in [6] with the solution in Section III-B for the case $N = 1$. For the zero-mean case (as in [6]), the linearity constraint is no longer needed and the solution takes the form of (17). Also, zero-mean processes imply that the covariances and the correlations are identical. This leads to

$$g^* = \frac{1}{\gamma} \frac{\sigma_{xy}}{\sigma_y^2} = \frac{1}{\gamma} \left(\frac{\sigma_x^2}{\sigma_x^2 + \sigma_\eta^2} \right). \tag{20}$$

In [6], we obtained the solution

$$g^* = \frac{-C_2 \sigma_y^2 + \sqrt{C_2^2 \sigma_y^4 + 4\sigma_x^2 \sigma_y^2 \left(\sigma_x^4 + C_2 \sigma_x^2 \right)}}{2\sigma_x^2 \sigma_y^2}. \tag{21}$$

The equivalence of the two solutions is shown Fig. 4. The plot compares the solution in (20) and the solution in [6]. The difference between the red ($*$) and green ($\diamond$) plots is less than 0.001, which is the value of ϵ chosen for this simulation.

IV. APPLICATION TO IMAGE DENOISING AND RESTORATION

While the SSIM index can be used to measure the quality of any two signals, it was originally designed for full-reference image quality assessment. With this in mind, we apply our solution to both an image denoising and a restoration problem.

The image restoration algorithm is summarized in the following steps (also applicable for denoising).

- At every pixel in the distorted image, form a neighborhood of size $N \times N$. The value of N depends on the number of samples needed to compute stable correlation values. From this neighborhood, form estimates of $\mathbf{r}_{xy}, \mathbf{c}_{xy}, \mathbf{R}_{yy}, \mathbf{K}_{yy}$.
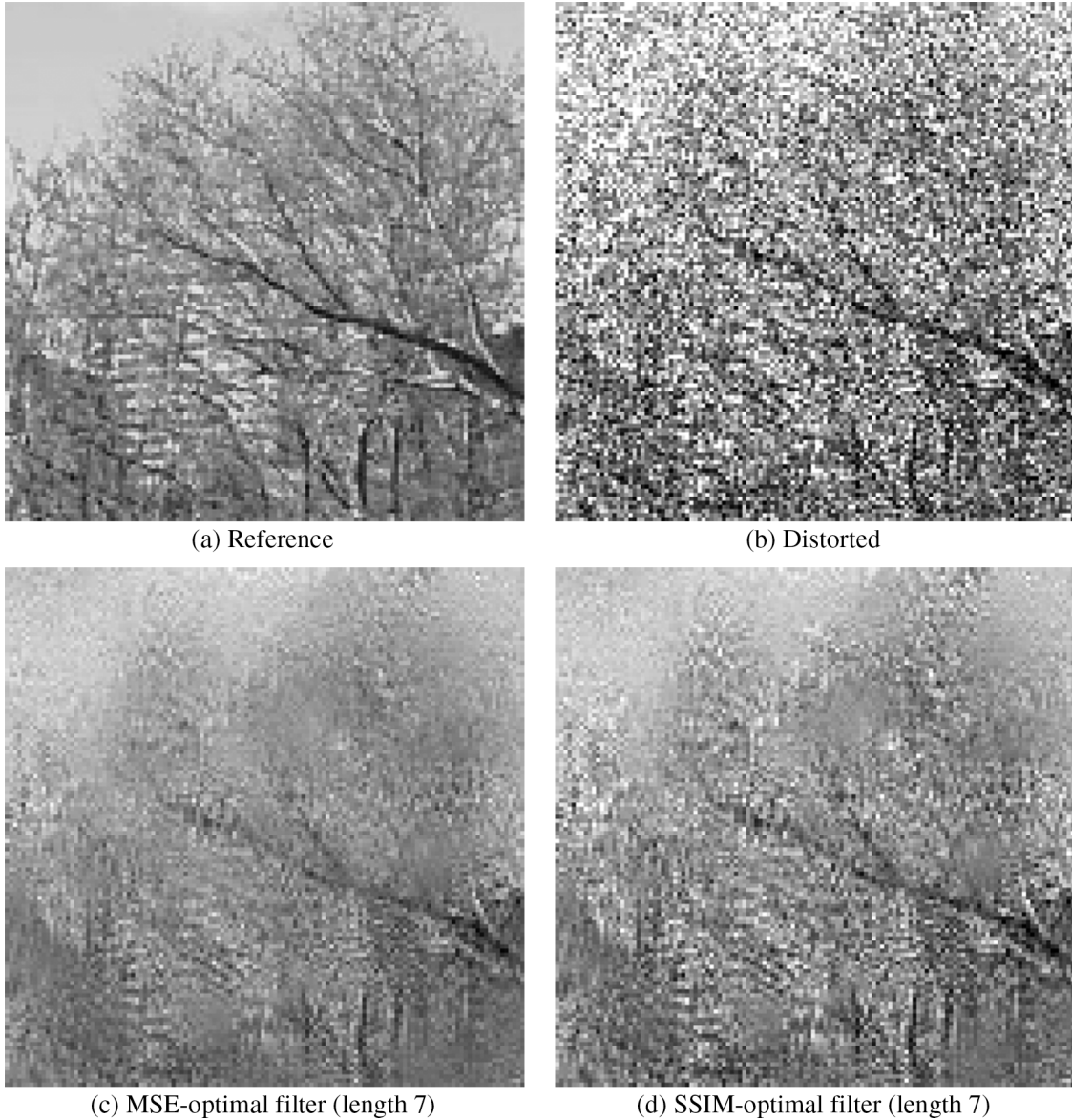
(a) Reference

(b) Distorted

(c) MSE-optimal filter (length 7)

(d) SSIM-optimal filter (length 7)

Fig. 7. *Denoising example 3*: (a) Original image. (b) Distorted image with $\sigma_{\text{noise}} = 50$, $\text{MSE} = 2461.8462$, $\text{SSIM index} = 0.3713$. (c) Image denoised with the a 7-tap MSE-optimal filter, $\text{MSE} = 616.2075$, $\text{SSIM index} = 0.4103$. (d) Image denoised with a 7-tap SSIM-optimal filter, $\text{MSE} = 786.7991$, $\text{SSIM index} = 0.4422$.

- The local Wiener solution is computed as $\mathbf{g}^*_{\text{mse}} = \mathbf{R}_{yy}^{-1}\mathbf{r}_{xy}$ (applied to zero-mean blocks).
- The following steps are used to compute the StatSSIM-optimal solution.
  — Compute the initial search point for α using the solution in (17).
  — For a range of α about the initial search point, compute the solution in (15) and pick the one that has the maximum StatSSIM index.

In this paper, we assume that the blurring filter and the power spectral density of the additive noise component is known at the receiver [18], [20]. The procedure used to estimate the correlation and covariance values for denoising and restoration is discussed below. For both cases, the neighborhood of size $N \times N$ is unwrapped into a vector of size $N^2 \times 1$, and the statistics are computed from this vector. We do this to be consistent with the way the SSIM index computes the local statistics in its implementation.

A. Denoising

The cross-covariance values at each pixel location are computed from the $N^2 \times 1$ vector formed from a local neighborhood around the given pixel of the observed image. The following relations are used in the computation:

$$
\begin{aligned}
c_{yy}(0) &= E\left[\left(y[n] - \mu_y\right)^2\right] \\
&= E\left[\left(x[n] + \eta[n] - \mu_y\right)^2\right] \\
&= c_{xx}(0) + \sigma_\eta^2 \\
\Rightarrow c_{xx}(0) &= c_{yy}(0) - \sigma_\eta^2.
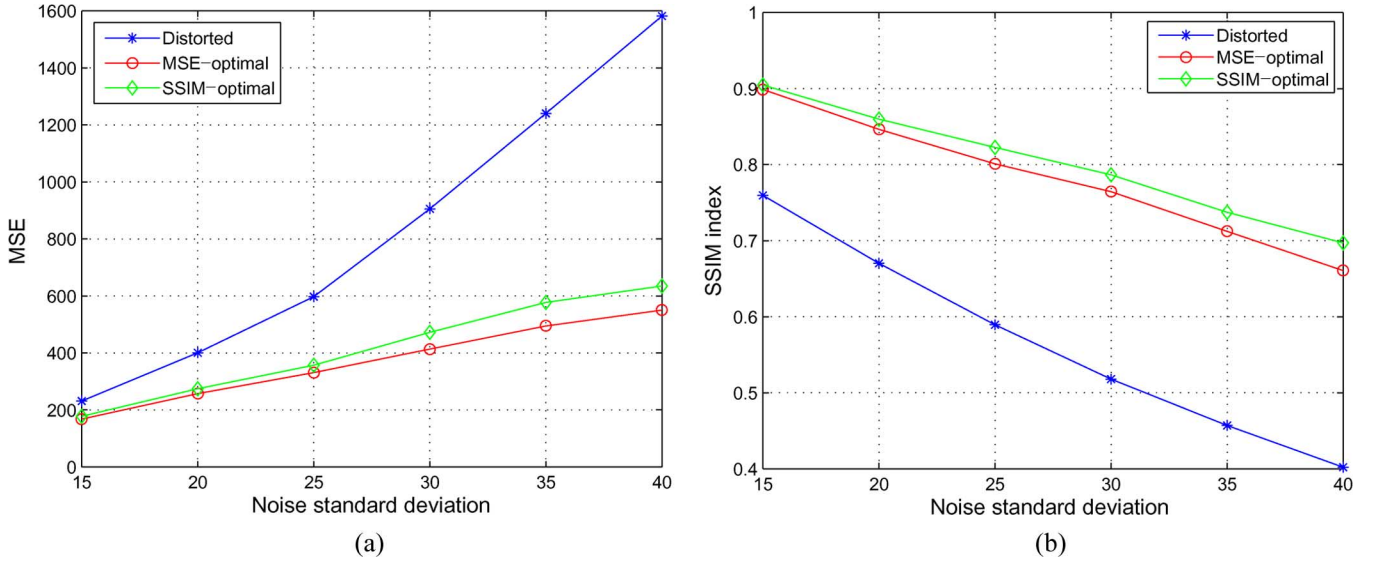\end{aligned} \tag{22}
$$

Fig. 8. For a 64×64 patch from Img0039.bmp from the "City of Austin" database, distorted with AWGN and restored using 5-tap MSE-optimal and SSIM-optimal filters. (a) Variation of denoised images' MSE with noise standard deviation. (b) Variation of denoised images' SSIM index with noise standard deviation.
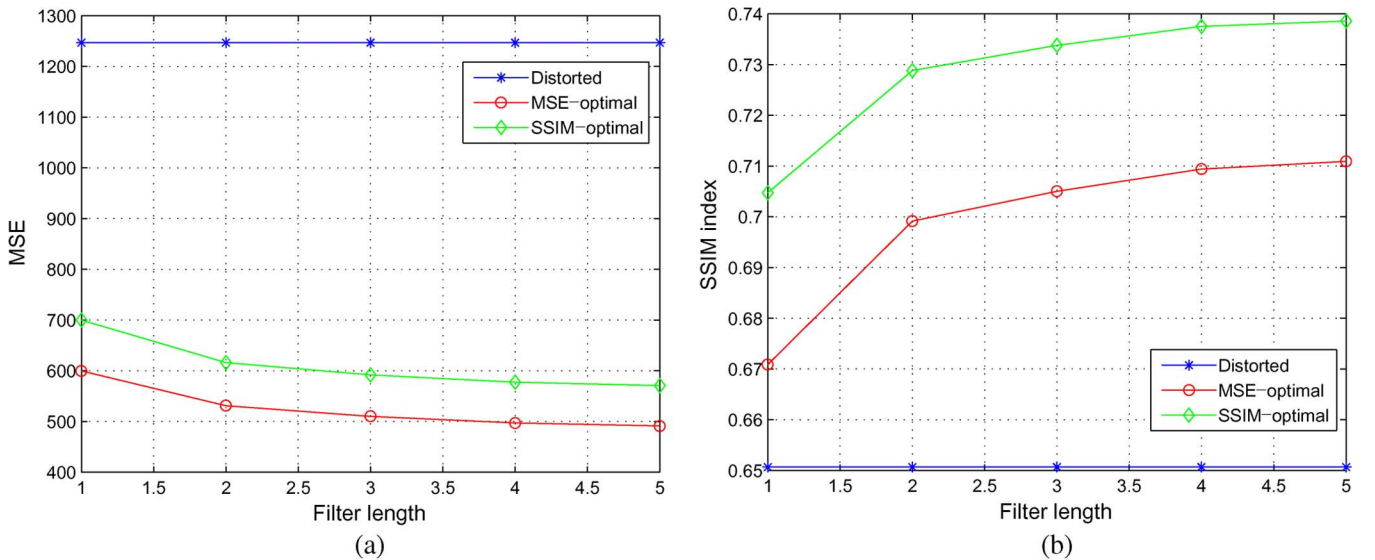

Fig. 9. For a 64×64 patch from Img0039.bmp from the "City of Austin" database, distorted with AWGN at $\sigma_{\text{noise}} = 35$. (a) Variation of denoised images' MSE with filter length. (b) Variation of denoised images' SSIM index with filter length.

The first equality holds since the noise is zero-mean; therefore, $\mu_y = \mu_x$, and the noise is independent of the source. Similarly, for $\tau \neq 0$

$$
\begin{aligned}
c_{yy}(\tau) &= E\left[(y[n] - \mu_y)(y[n-\tau] - \mu_y)\right] \\
&= E\left[(x[n] + \eta[n] - \mu_x) \right. \\
&\qquad \left. \times (x[n-\tau] + \eta[n-\tau] - \mu_x)\right] \\
&= c_{xx}(\tau), \\
\Rightarrow c_{xy}(\tau) &= E\left[(x[n] - \mu_x)(y[n-\tau] - \mu_y)\right] \\
&= E\left[(x[n] - \mu_x)(x[n-\tau] - \mu_y + \eta[n-\tau])\right] \\
&= c_{xx}(\tau) = c_{yy}(\tau).
\end{aligned}
\tag{23}
$$

The first equality relation holds since $\eta[n]$ and $\eta[n-\tau]$ are independent (of each other, and the source process $x[n]$) and

zero-mean. The second equality relation easily follows from the first.

B. Restoration

The estimation of the cross covariance is not as straightforward for the case of restoration, as it involves inversion of blurring kernels whose inverses are usually very unstable. Portilla and Simoncelli [20] proposed a heuristic technique for estimating the cross covariance between the observed image and the original for an image restoration application. In this paper, we follow their approach with minor modifications. The 2-D equivalent for the model shown in Fig. 1 can be expressed as

$$
y(m, n) = h(m, n) * x(m, n) + \eta(m, n)
\tag{24}
$$

(a) Reference

(b) Distorted

(c) MSE-optimal filter

(d) StatSSIM-optimal filter

Fig. 10. *Restoration example 1*: Image Img0073.bmp of the "City of Austin" database. (a) Original image. (b) Distorted image with $\sigma_{\text{blur}} = 15$, $\sigma_{\text{noise}} = 40$, $\text{MSE} = 2264.4425$, $\text{SSIM index} = 0.3250$. (c) Image restored with a 11-tap MSE-optimal filter, $\text{MSE} = 955.6455$, $\text{SSIM index} = 0.3728$. (d) Image restored with a 11-tap SSIM-optimal filter, $\text{MSE} = 1035.0551$, $\text{SSIM index} = 0.4215$.

where $h(m, n)$ is the blurring kernel, $x(m, n)$ is the reference image, and $\eta(m, n)$ is zero-mean white Gaussian noise (independent of $x(m, n)$) of known power spectral density $P_\eta(u, v)$. It is easy to show that the cross covariance between $y(m, n)$ and $x(m, n)$ is equal to the cross covariance between $x'(m, n)$ and $x(m, n)$, where $x'(m, n) = h(m, n) * x(m, n)$, since $x(m, n)$ and $\eta(m, n)$ are independent, and $\eta(m, n)$ is zero-mean. Also, from (24), the relation between the PSD of the observed image and the original is $P_y(u, v) = P_x(u, v)|H(u, v)|^2 + P_\eta(u, v)$. This relation is used to estimate the PSD of $x'(m, n)$ as

$$P_{x'}(u, v) \approx \left\lfloor |Y(u, v)|^2 - P_\eta(u, v) \right\rfloor_+ . \tag{25}$$

The PSD of the original image is then estimated as

$$P_x(u, v) \approx P_{x'}(u, v) / \max\left(|H(u, v)|^2, k\right) \tag{26}$$

where k is a constant used to prevent instability during the channel inversion process. The value of k is chosen empirically for each image, at a given blur and noise variance. In our experiments we found that $k = 3$ gave us good results. The cross correlation between $x(m, n)$ and $x'(m, n)$ is computed as the sample cross covariance of the inverse Fourier transform coefficients of $\sqrt{P_x(u, v)}$ and $\sqrt{P_{x'}(u, v)}$. The inverse Fourier transform coefficients (of $\sqrt{P_x(u, v)}$ and $\sqrt{P_{x'}(u, v)}$) are unwrapped into vectors and the cross-covariance values are computed from them.

V. RESULTS

In this section, we present the results of the StatSSIM-optimal image denoising and restoration procedures and compare the performance to the local MSE-optimal denoising and restoration procedures. The *local* MSE-optimal filter is a powerful
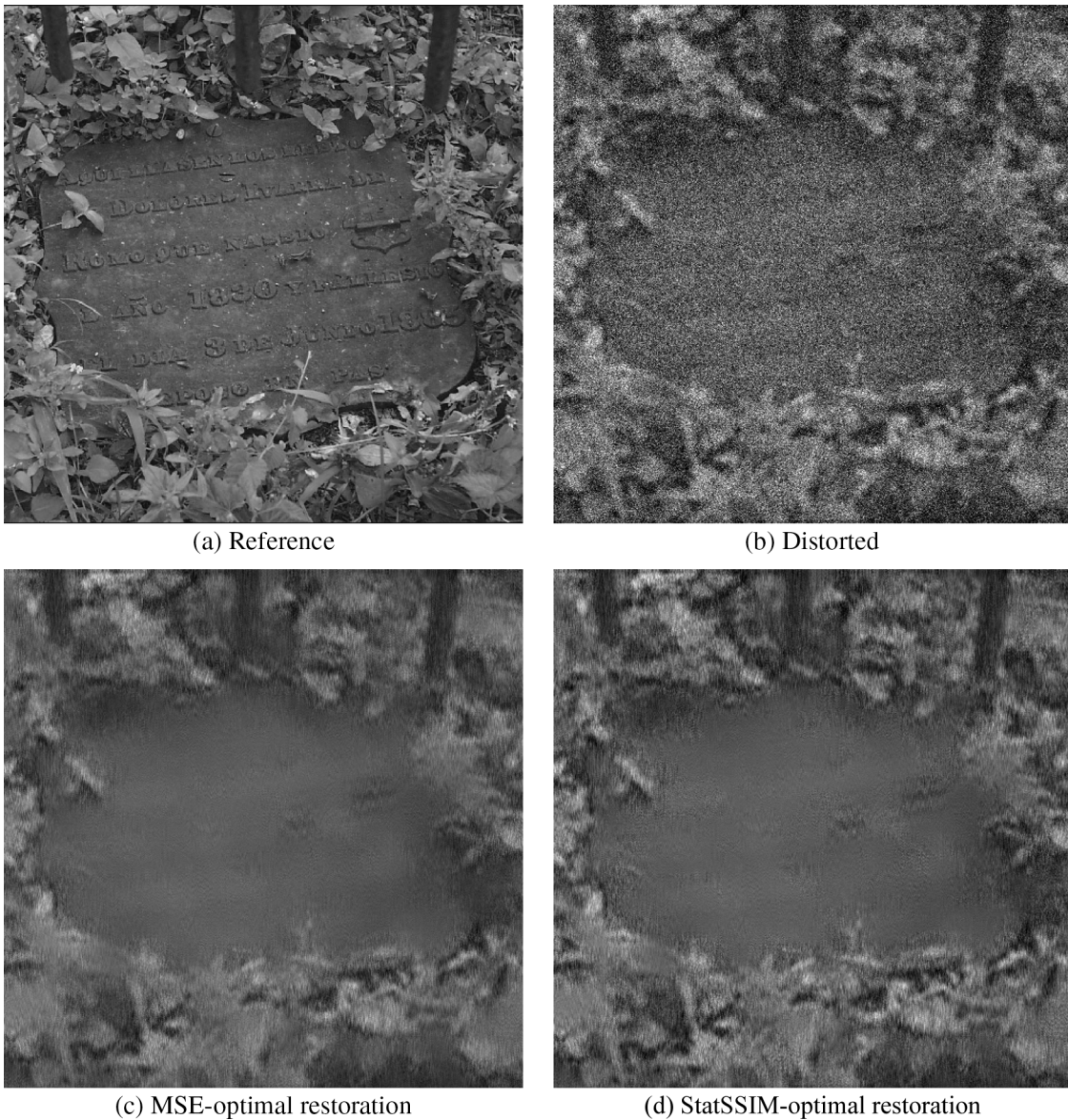
(a) Reference

(b) Distorted

(c) MSE-optimal restoration

(d) StatSSIM-optimal restoration

Fig. 11.   *Restoration example 2*: Image Img00124.bmp of the "City of Austin" database. (a) Original image. (b) Distorted image with $\sigma_{\mathrm{blur}} = 5, \sigma_{\mathrm{noise}}^2 = 1600$, $\mathrm{MSE} = 2014.5695, \mathrm{SSIM}$ index $= 0.2878$. (c) Image restored with a 11-tap MSE-optimal filter, $\mathrm{MSE} = 681.0735, \mathrm{SSIM}$ index $= 0.3769$. (d) Image restored with a 11-tap SSIM-optimal filter, $\mathrm{MSE} = 738.8895, \mathrm{SSIM}$ index $= 0.4131$. Note the better contrast in the leaves.

linear filter due to its local-adaptation. The denoising results are presented first, followed by the restoration results. We demonstrate that the perceptual quality of the StatSSIM-optimally denoised and restored images is superior to the MSE-optimally denoised and restored images. The results presented here are from a *pixel domain* implementation of the solutions.

A. Denoising Results

The denoising solution was applied to natural images that have been corrupted with zero-mean additive white gaussian noise (AWGN). The cross-correlation and cross-covariance values needed by the solutions are estimated using the technique presented in Section IV-A. A neighborhood size of 15×15 is used in our implementation. The solution was tested on several images from the "City of Austin" database, and on standard test images such as Lena, Barbara, and Boats. The results for 7-tap MSE-optimal and StatSSIM-optimal filters are shown in Fig. 5 for an image from the "City of Austin" database. Both the MSE-optimal and the StatSSIM-optimal solutions have been applied to neighborhoods with their mean removed (zero-mean blocks). The local means are added back after filtering. From Fig. 5, we see that the StatSSIM-optimal solution retains more image features (e.g., the branches, and building details obscured by branches) than the MSE-optimal solution. The MSE-solution on the other hand, performs denoising irrespective of the image features. This result manifests itself in lower MSE values for the MSE-optimal filter, and higher SSIM indices for the StatSSIM-optimal filter. Fig. 6 shows a region of the Lena image that has been corrupted with noise and denoised using the MSE-optimal and SSIM-optimal techniques. From
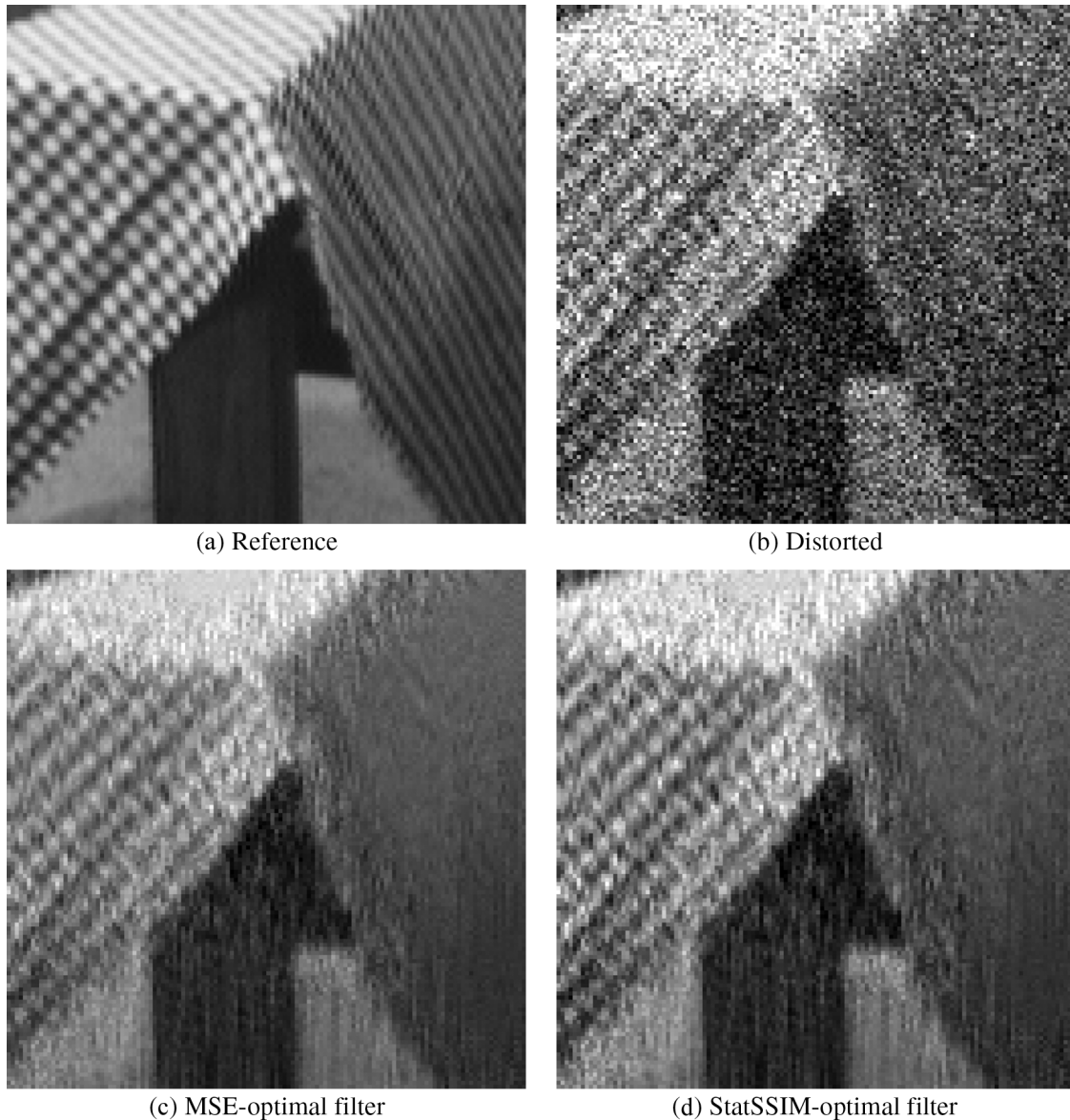
(a) Reference

(b) Distorted

(c) MSE-optimal filter

(d) StatSSIM-optimal filter

Fig. 12. *Restoration example 3*: A 128×128 block of Barbara image. (a) Original image. (b) Distorted image with $\sigma_{\mathrm{blur}} = 1, \sigma_{\mathrm{noise}} = 40, \mathrm{MSE} = 1781.9058$, SSIM index $= 0.5044$. (c) Image restored with a 11-tap MSE-optimal filter, $\mathrm{MSE} = 520.1322$, SSIM index $= 0.6302$. (d) Image restored with a 11-tap SSIM-optimal filter, $\mathrm{MSE} = 584.9232$, SSIM index $= 0.6568$.

this example, it can be seen that the SSIM-optimal technique retains more details in the high frequency region of the image (Lena's hair) and has a higher overall contrast compared to the MSE-optimal method. Fig. 7 shows the comparison for a region of the "Img0039.bmp" image. Again, the SSIM-optimal method does a better job at retaining image features as seen in the better visibility of the building in the background and lower smoothing of the branches. The plot of the variation of the MSE and SSIM index of the noisy and denoised images as a function of the noise variance is shown in Fig. 8. Further, since our solution can be used to obtain optimal filters of any length N, we plot the variation of MSE and SSIM index as a function of the filter length in Fig. 9. As expected, the performance of both the algorithms improves with filter length. Also, a clear

knee is observed in the plot, which gives a good estimate of the filter length needed at that particular noise value.

B. Restoration Results

The restoration solution was applied to natural images that have been blurred using a Gaussian kernel, and corrupted with AWGN. The estimation of the cross-covariance vector needed by the solutions is done using the procedure outlined in Section IV-B. We present examples at various blur values in Figs. 10–14. In all the examples, the size of the blurring kernel used is 7×7, and a 11-tap restoration filter is used. We note that solving for a 11-tap SSIM-optimal filter (even globally) by brute force is highly intractable.
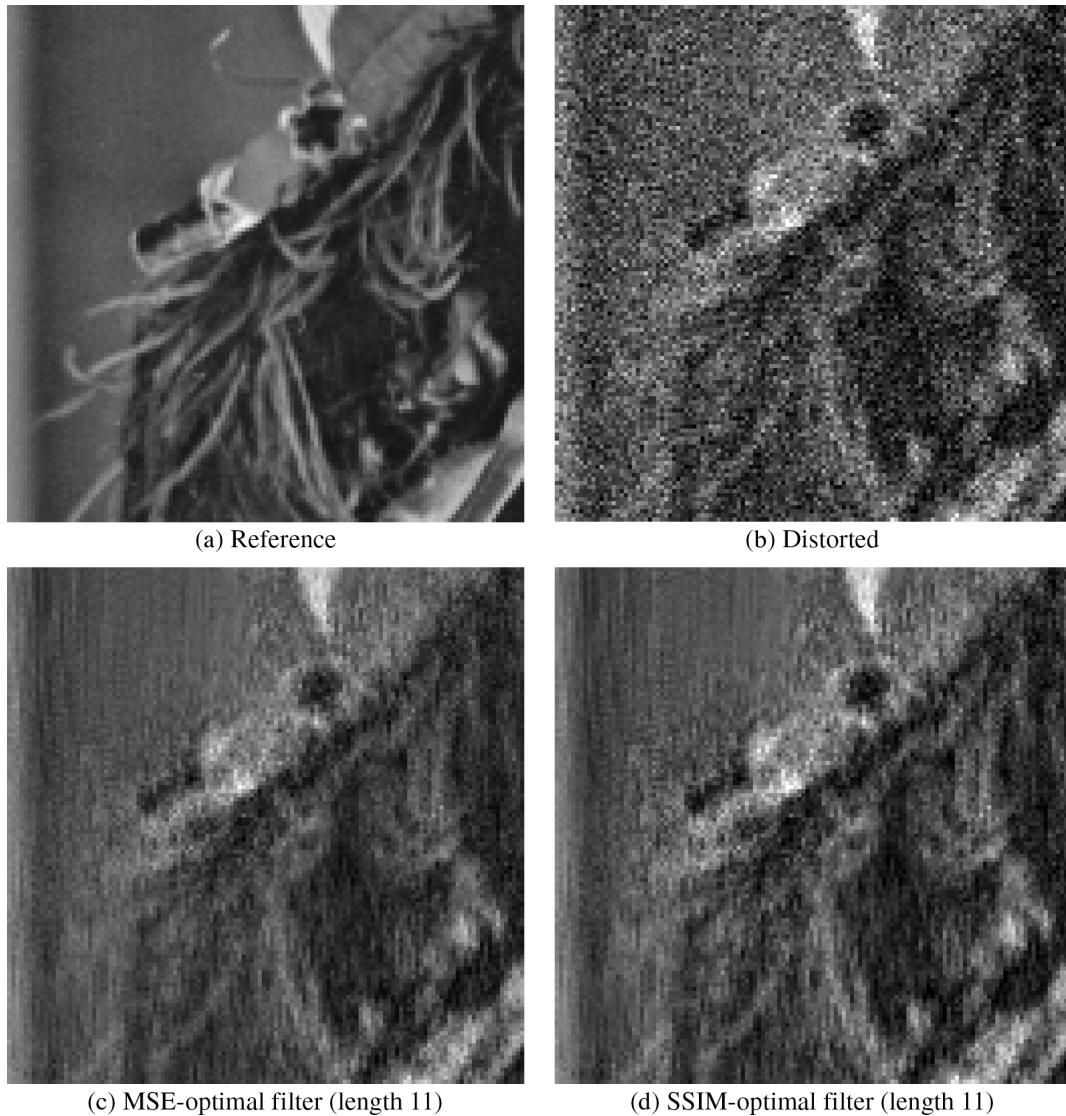
(a) Reference

(b) Distorted

(c) MSE-optimal filter (length 11)

(d) SSIM-optimal filter (length 11)

Fig. 13. *Restoration example 4*: (a) Original image. (b) Distorted image with $\sigma_{\text{blur}} = 1, \sigma_{\text{noise}} = 30, \text{MSE} = 980.9643, \text{SSIM index} = 0.611074.$ (c) Image restored with the a 11-tap MSE-optimal filter, $\text{MSE} = 364.5094, \text{SSIM index} = 0.759695.$ (d) Image restored with a 11-tap SSIM-optimal filter, $\text{MSE} = 453.9657, \text{SSIM index} = 0.763995.$

The higher perceptual quality of the StatSSIM-optimally restored images as compared to MSE-optimally restored images is evident from these examples. In Fig. 10, the SSIM-optimally restored image has better contrast overall, with noticeable differences in the foliage, and the rocks. In Fig. 11, SSIM-optimal restoration helps retain more detail in the leafy regions of the image and has better contrast. In Fig. 12, the SSIM-optimal restoration does a better job on the checked pattern on the table cloth compared to MSE-optimal restoration. In both Figs. 13 and 14, the SSIM-optimal solution preserves more detail in Lena's hair and has a higher overall contrast.

The variation of MSE and SSIM index as a function of the noise standard deviation is present in Fig. 15. From the trend, we see that the performance of the two algorithms can be clearly distinguished, increasingly so with increasing noise variance. The intuition behind this trend can be understood with the example of a 1-tap filter. In this case, for a zero-mean source, the MSE-optimal filter is $g_{\text{mse}} = c_{xy}[0]/c_{yy}[0]$, and a simplified SSIM-optimal filter (with $C_2 = 0$) in closed-form is $g_{\text{ssim}} = \sqrt{c_{xy}[0]/c_{yy}[0]}$. The square root relation between the two solutions explains the trend observed in Fig. 15. The variation of the performance with filter length is illustrated in Fig. 16. As with denoising, the trend is an improvement with filter length.

An important point to note is that the performance of both the algorithms is dependent on the quality of the estimates of the cross correlations and cross covariances. For both these cases, a neighborhood size of 35×35 is used to compute the required statistics. The implementation in this paper is based on the heuristic technique presented in [20], and this can be improved further. For example, using an iterative algorithm as in [13] is a promising alternative to the heuristic approach.
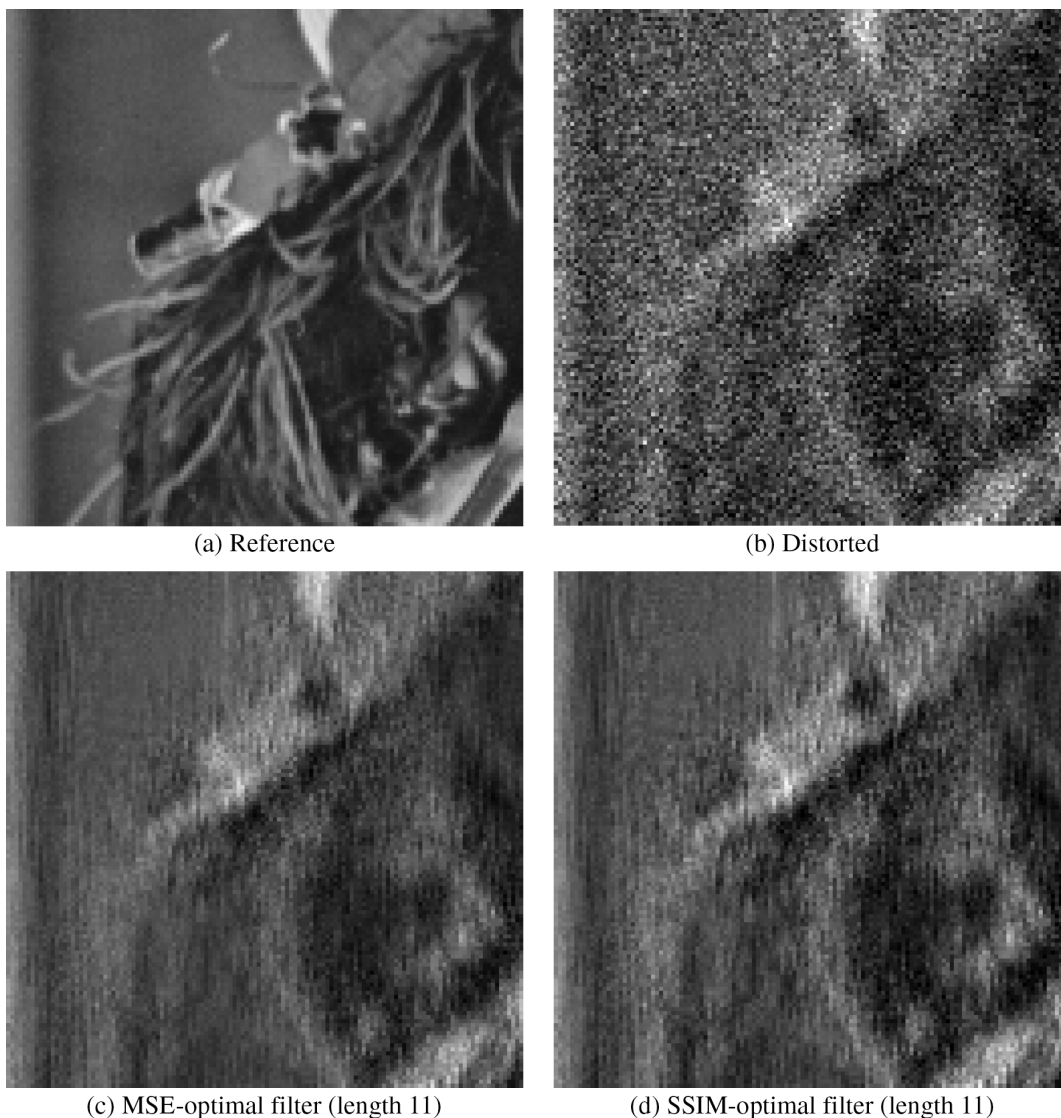
Fig. 14. *Restoration example 5*: (a) Original image. (b) Distorted image with $\sigma_{\text{blur}} = 5$, $\sigma_{\text{noise}} = 30$, $\text{MSE} = 1216.4048$, $\text{SSIM index} = 0.506031$. (c) Image restored with the a 11-tap MSE-optimal filter, $\text{MSE} = 528.2466$, $\text{SSIM index} = 0.654534$. (d) Image restored with a 11-tap SSIM-optimal filter, $\text{MSE} = 620.4033$, $\text{SSIM index} = 0.670088$.

C. Discussion

The design of the StatSSIM-optimal equalizer was motivated by the fact that the SSIM index is a better perceptual image quality metric than the ubiquitous MSE measure. From the denoising and deblurring results, it is clear that optimizing for a perceptual distortion measure is more meaningful for image data. The gain in image quality can be explained as follows: the StatSSIM-optimal solution strives to maximize the local mean, variance, and structure in the denoised and restored images, with respect to the reference. The local MSE-optimal solution, on the other hand, does not differentiate between the signal and the noise, thereby resulting in smoothing of important structural information while denoising and restoring images.

The SSIM index can be used to measure the quality of test signals with respect to the reference not just for images, but also for 1-D and higher dimensional signals. While the SSIM-optimal solution presented here has been applied to image denoising

and restoration examples, the solution can be applied as-is or extended to equalization problems in digital communications, speech processing, system identification, etc.

VI. CONCLUSION AND FUTURE WORK

In this paper, we formulated and solved a linear equalization problem optimized for the StatSSIM index. The nonconvex problem was first transformed to a convex one by applying a parameterized linearity constraint. The optimal solution was found by performing a search over the linearity constraint parameter. To the best of our knowledge, this is the first such attempt at an optimization for the SSIM index. To demonstrate the usefulness of the algorithm, it was applied to image denoising and restoration problems. The results of denoising and restoration clearly showed a gain in perceptual quality achieved by using the StatSSIM-optimal equalization algorithm.

The results in this paper depend on the accuracy of the estimation of the cross-correlation and cross-covariance values. These
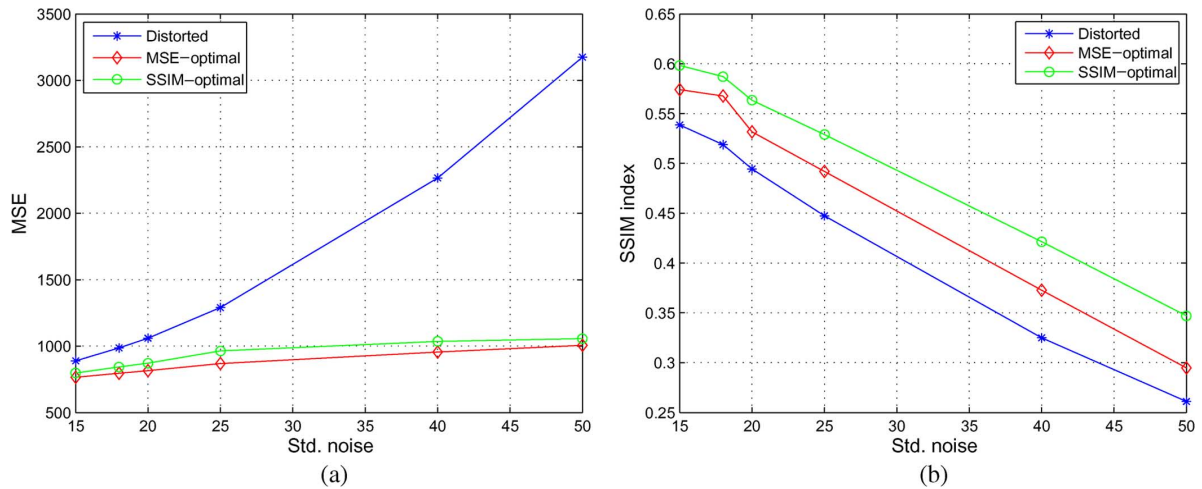
Fig. 15. For Img0073.bmp from the "City of Austin" database, distorted with $\sigma_{\mathrm{blur}} = 15$, and restored using a 11-tap filter. (a) Plot of MSE versus noise standard deviation σ_{noise}. (b) Plot of SSIM index versus noise standard deviation σ_{noise}.
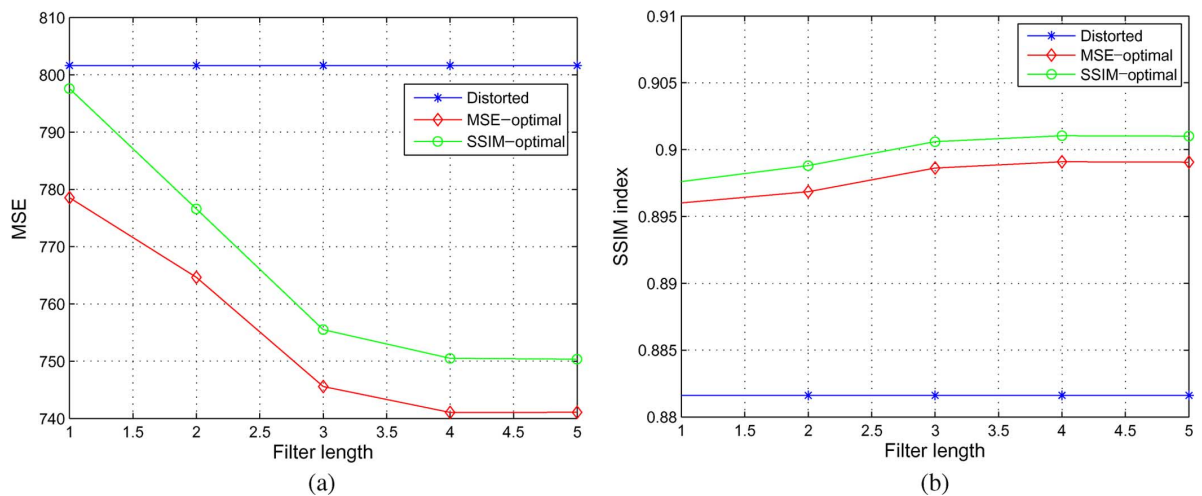

Fig. 16. For a 64 × 64 patch from Img0099.bmp from the "City of Austin" database, distorted with $\sigma_{\mathrm{blur}} = 1$, and corrupted with $\sigma_{\mathrm{noise}} = 12$. (a) Plot of MSE versus filter length. (b) Plot of SSIM index versus filter length.

can clearly be improved by using more sophisticated estimation techniques than the heuristic technique currently being used. The results in this paper open up several interesting avenues for optimization with respect to the SSIM index. While a linear filter was designed here, we are currently working on a more general solution that maximizes the SSIM index without the linearity restriction. Further, the current solution is implemented in the image domain. Extending this approach to a multiscale domain, such as the wavelet domain, appears very promising. SSIM-optimal designs can also be carried out for other important applications such as motion-estimation and compensation, multiframe reconstruction, rate allocation for image coding, to name a few.

REFERENCES

[1] H. C. Andrews and B. R. Hunt, *Digital Image Restoration*. Englewood Cliffs, NJ: Prentice-Hall, 1977.

[2] M. R. Banham and A. K. Katsaggelos, "Spatially adaptive wavelet-based multiscale image restoration," *IEEE Trans. Image Process.*, vol. 5, no. 4, pp. 619–634, Apr. 1996.

[3] D. P. Bertsekas, *Nonlinear Programming*. Belmont, MA: Athena, 1995.

[4] S. Boyd and L. Vandenberghe, *Convex Optimization*. Cambridge, U.K.: Cambridge Univ. Press, 2004.

[5] D. M. Chandler and S. S. Hemami, *VSNR: A Wavelet-Based Visual Signal-to-Noise Ratio for Natural Images*. private communication.

[6] S. S. Channappayya, A. C. Bovik, and R. W. Heath, Jr., "A linear estimator optimized for the structural similarity index and its application to image denoising," in *Proc. IEEE Int. Conf. Image Processing*, 2006, vol. 3, pp. 2637–2640.

[7] S. Daly, "The visible difference predictor: An algorithm for the assessment of image fidelity," in *Digital Images and Human Vision*, A. B. Watson, Ed. Cambridge, MA: MIT Press, 1993, pp. 179–206.

[8] D. L. Donoho, "Nonlinear solution of linear inverse problems by wavelet-vaguelette decomposition," *Appl. Comput. Harmon. Anal.*, vol. 2, no. 2, pp. 101–126, 1995.

[9] J. D. Eggerton and M. D. Srinath, "A visually weighted quantization scheme for image bandwidth compression at low data rates," *IEEE Trans. Commun.*, vol. COM-34, pp. 840–847, Aug. 1986.

[10] M. A. T. Figueiredo and R. D. Nowak, "An EM algorithm for wavelet-based image restoration," *IEEE Trans. Image Process.*, vol. 12, no. 8, pp. 906–916, Aug. 2003.

[11] B. Girod, "What's wrong with mean-squared error?," in *Digital Images and Human Vision*, A. B. Watson, Ed. Cambridge, MA: MIT Press, 1993, pp. 207–220.

[12] L. Guan and R. K. Ward, "Restoration of randomly blurred images by the Wiener filter," *IEEE Trans. Signal Process.*, vol. 37, no. 4, pp. 589–592, Apr. 1988.

[13] A. D. Hillery and R. T. Chin, "Iterative Wiener filters for image restoration," *IEEE Trans. Signal Process.*, vol. 39, no. 8, pp. 1892–1899, Aug. 1991.

[14] A. K. Katsaggelos, Ed.*, Digital Image Restoration.* Berlin, Germany: Springer-Verlag, 1991.

[15] R. L. Lagendijk, J. Biemond, and D. E. Boekee, "Regularized iterative image restoration with ringing reduction," *IEEE Trans. Signal Process.*, vol. 36, no. 12, pp. 1874–1888, Dec. 1988.

[16] J. Lubin, "The use of psychophysical data and models in the analysis of display system performance," in *Digital Images and Human Vision*, A. B. Watson, Ed. Cambridge, MA: MIT Press, 1993, pp. 163–178.

[17] J. L. Mannos and D. J. Sakrison, "The effects of a visual fidelity criterion on the encoding of images," *IEEE Trans. Inf. Theory*, vol. 20, no. 4, pp. 525–536, Jul. 1974.

[18] R. Neelamani, H. Choi, and R. Baraniuk, "ForWaRD: Fourier-wavelet regularized deconvolution for ill-conditioned systems," *IEEE Trans. Signal Process.*, vol. 52, no. 2, pp. 418–433, Feb. 2004.

[19] N. B. Nill, "A visual model weighted cosine transform for image compression and quality assessment," *IEEE Trans. Commun.*, vol. 33, no. 4, pp. 551–557, Jul. 1985.

[20] J. Portilla and E. P. Simoncelli, "Image restoration using Gaussian scale mixtures in the wavelet domain," in *Proc. IEEE Int. Conf. Image Processing.*, 2003, vol. 2, pp. 965–968.

[21] S. J. Reeves, "Optimal space-varying regularization in iterative image restoration," *IEEE Trans. Image Process.*, vol. 3, no. 3, pp. 319–324, Mar. 1994.

[22] H. R. Sheikh and A. C. Bovik, "Image information and visual quality," *IEEE Trans. Image Process.*, vol. 15, no. 2, pp. 430–444, Feb. 2006.

[23] H. R. Sheikh, A. C. Bovik, and G. de Veciana, "An information fidelity criterion for image quality assessment using natural scene statistics," *IEEE Trans. Image Process.*, vol. 14, no. 12, pp. 2117–2128, Dec. 2005.

[24] H. R. Sheikh, M. F. Sabir, and A. C. Bovik, "A statistical evaluation of recent full reference image quality assessment algorithms," *IEEE Trans. Image Process.*, vol. 15, no. 11, pp. 3440–3451, Nov. 2006.

[25] P. C. Teo and D. J. Heeger, "Perceptual image distortion," *Proc. SPIE*, vol. 2179, pp. 127–141, 1994.

[26] Z. Wang and A. C. Bovik, "A universal image quality index," *IEEE Signal Process. Lett.*, vol. 9, no. 3, pp. 81–84, Mar. 2002.

[27] Z. Wang, A. C. Bovik, H. R. Sheikh, and E. P. Simoncelli, "Image quality assessment: From error visibility to structural similarity," *IEEE Trans. Image Process.*, vol. 13, no. 4, pp. 600–612, Apr. 2004.

[28] Z. Wang, Q. Li, and X. Shang, "Perceptual image coding based on a maximum of minimal structural similarity criterion," presented at the IEEE Int. Conf. Image Processing, Sep. 2007.

[29] Z. Wang and E. P. Simoncelli, "Translation insensitive image similarity in complex wavelet domain," in *Proc. IEEE Int. Conf. Acoustics, Speech, and Signal Processing*, 2005, vol. 2, pp. 573–576.

[30] Z. Wang, E. P. Simoncelli, and A. C. Bovik, "Multi-scale Structural similarity for image quality assessment," presented at the IEEE Asilomar Conf. Signals, Systems and Computers., 2003.

[31] A. B. Watson, "Visually optimal DCT quantization matrices for individual images," in *Proc. Data Compression Conf.*, Mar. 30–Apr. 2, 1993, pp. 178–187.

[32] A. B. Watson*, Digital Images and Human Vision.* Cambridge, MA: MIT Press, 1993.

[33] S. Winkler, "A perceptual distortion mertic for digital color video," in *Proc. SPIE*, 1999, vol. 3644, pp. 175–184.
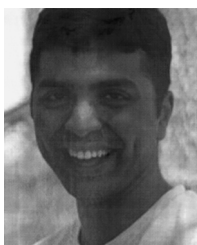
Sumohana S. Channappayya (S'01–M'08) received the B.E. degree from the University of Mysore, India, in 1998, the M.S. degree in electrical engineering from the Arizona State University, Tempe, in 2000, and the Ph.D. degree in electrical and computer engineering from The University of Texas at Austin in 2007.

He is currently with PacketVideo Corporation, San Diego, CA. His research interests include image restoration, image and video coding, image and video quality assessment, and multimedia communication.
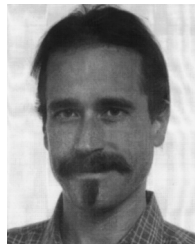
Alan Conrad Bovik (S'80–M'81–SM'89–F'96) received the B.S., M.S., and Ph.D. degrees in electrical and computer engineering from the University of Illinois, Urbana-Champaign, in 1980, 1982, and 1984, respectively.

He is currently the Curry/Cullen Trust Endowed Professor at the University of Texas, Austin, where he is the Director of the Laboratory for Image and Video Engineering (LIVE) in the Center for Perceptual Systems. His research interests include image and video processing, computational vision, digital microscopy, and modeling of biological visual perception. He has published over 450 technical articles in these areas and holds two U.S. patents. He is the author of *The Handbook of Image and Video Processing*, 2nd ed. (Elsevier Academic Press, 2005) and *Modern Image Quality Assessment* (Morgan & Claypool, 2006).

Dr. Bovik has received a number of major awards from the IEEE Signal Processing Society, including: the Education Award (2007), the Technical Achievement Award (2005), the Distinguished Lecturer Award (2000), and the Meritorious Service Award (1998). He is also a recipient of the IEEE Third Millennium Medal (2000), and a two-time Honorable Mention winner of the international Pattern Recognition Society Award for Outstanding Contribution (1988 and 1993). He is a Fellow of the Optical Society of America. He has been involved in numerous professional society activities, including: Board of Governors, IEEE Signal Processing Society, 1996–1998; Editor-in-Chief, IEEE TRANSACTIONS ON IMAGE PROCESSING, 1996–2002; Editorial Board, THE PROCEEDINGS OF THE IEEE, 1998–2004; Series Editor for *Image, Video, and Multimedia Processing*, Morgan & Claypool Publishing Company, 2003-present; and Founding General Chairman, First IEEE International Conference on Image Processing, held in Austin, TX, in November 1994. Dr. Bovik is a Registered Professional Engineer in the State of Texas and is a frequent consultant to legal, industrial, and academic institutions.
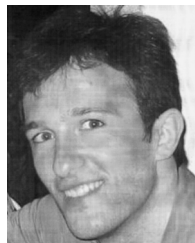
Constantine Caramanis (S'05–M'06) received the B.A. degree in mathematics from Harvard University, Cambridge, MA, in 1999, and the M.S. and Ph.D. degrees in electrical engineering and computer science from the Massachusetts Institute of Technology, Cambridge, in 2001 and 2006, respectively.

He is currently an Assistant Professor of electrical and computer engineering at The University of Texas at Austin. His research interests include stochastic, robust, and adaptable optimization and control, convex and combinatorial optimization, learning theory, and applications to communications, networks, and scheduling.

Robert W. Heath, Jr. (S'96–M'01–SM'06) received the B.S. and M.S. degrees from the University of Virginia, Charlottesville, in 1996 and 1997, respectively, and the Ph.D. degree from Stanford University, Stanford, CA, in 2002, all in electrical engineering.

From 1998 to 2001, he was a Senior Member of the Technical Staff, then a Senior Consultant, at Iospan Wireless, Inc., San Jose, CA, where he worked on the design and implementation of the physical and link layers of the first commercial MIMO-OFDM communication system. In 2003, he founded MIMO Wireless, Inc., a consulting company dedicated to the advancement of MIMO technology. Since January 2002, he has been with the Department of Electrical and Computer Engineering, The University of Texas at Austin, where he is currently an Associate Professor and member of the Wireless Networking and Communications Group. His research interests include several aspects of MIMO communication: limited feedback techniques, multihop networking, multiuser MIMO, antenna design, and scheduling algorithms, as well as 60-GHz communication techniques and multimedia signal processing.

Dr. Heath has been an Editor of the IEEE TRANSACTIONS ON COMMUNICATIONS and an Associate Editor for the IEEE TRANSACTIONS ON VEHICULAR TECHNOLOGY. He is a member of the Signal Processing for Communications Technical Committee in the IEEE Signal Processing Society. He was a Technical Co-Chair for the 2007 Fall Vehicular Technology Conference, is the General Chair of the 2008 Communication Theory Workshop, and is a Co-Organizer of the 2009 Signal Processing for Wireless Communications Workshop. He is the recipient of the David and Doris Lybarger Endowed Faculty Fellowship in Engineering and is a Registered Professional Engineer in Texas.